Synthesis, Biological Testing, and Binding Mode Prediction of 6,9-Diarylpurin-8-ones as p38 MAP Kinase Inhibitors

Dominik R. J. Hauser,[†] Thomas Scior,[§] David M. Domeyer,[†] Bernd Kammerer,[‡] and Stefan A. Laufer*,[†]

Department of Pharmaceutical and Medicinal Chemistry, Eberhard-Karls-University Tübingen, Auf der Morgenstelle 8, 72076 Tübingen, Germany, Department of Clinical Pharmacology, University Hospital, Eberhard-Karls-University Tübingen, Otfried-Müller-Strasse 45, 72076 Tübingen, Germany, and Department of Pharmacy, Benemérita Universidad Autónoma de Puebla, 14 Sur con Avienda San Claudio, C.P. 72570 Puebla, México

Received September 7, 2006

Based on the purine scaffold of ATP, derivatives of 6,9-diarylpurine-8-one were prepared and tested for their ability to inhibit p38 MAP kinase, a key enzyme in the cellular regulation of proinflammatory cytokines. The inhibitor design combines the purine system of the authentic cosubstrate ATP with various phenyl moieties to explore the selectivity for the two hydrophobic regions of the kinase's ATP-binding cleft. The present study indicates a new binding mode of our scaffold to p38 MAP kinase, which comprises the desired structural features of ATP and the *N*-phenyl-*N*-purin-6-yl ureas previously published by Wan et al. Combinations of Autodock and FlexX docking with different scoring functions were used to assess the postulated binding mode. The predictive power of different docking-scoring combinations was determined. The presented results may form a solid basis for further optimization cycles since our theoretical findings are consistent with our experimental binding data and supported by the literature.

Introduction

The p38 MAP[a] kinase is closely associated with the cytokine-driven progression of rheumatoid arthritis and related inflammatory diseases. This enzyme tightly controls the expression of proinflammatory cytokines like IL-1β and TNFα at the levels of transcription and translation.[1] In human immune cells the p38 MAP kinase signaling pathway is activated in a self-inducing manner by cytokines.[2] Cellular activation of the pathway occurs *in vitro* in response to environmental stresses such as ultraviolet light, heat, osmotic shock, and inflammatory cytokines.[1] Due to its prominent role in regulating the production of inflammatory cytokines, the inhibition of p38 MAP kinase is an attractive approach for the treatment of cytokine-mediated diseases.[3]

Most of the p38 inhibitors published to date rely structurally on a vicinal diaryl system which provides selectivity.[4,5] As reported for many kinase inhibitors,[6] such molecules bind to p38 MAP kinase competitively with ATP. Molecular modeling allows the reproduction of the crystallographic binding modes of the natural ligand[7] and of the lead compounds SB 203580[8] or ML 3163,[5] which are typical inhibitors of the vicinal diaryl class (Figures 1 and 2). The first aryl, a 4-pyridyl moiety, mimics a conserved hydrogen bond, originally formed between N-1 of ATP and the backbone amide N−H of Met 109 (Figure 1).[5] The second aryl, a 4-fluorophenyl moiety occupies the kinase's hydrophobic region I which is pocket-shaped (Figure 2). Intriguingly, ATP does not occupy this hydrophobic region I (selectivity pocket) when bound to the kinase (Figure 1), thus providing opportunities for the design of selective inhibitors with an appropriate substitution pattern targeting region I and, in order to increase affinity, region II.[9] In a recent publication we presented compounds combining the purine system from the original cosubstrate ATP and phenyl moieties in order to explore possible interactions with the different regions of the ATP binding site in several disease-related protein kinases.[10] In this paper we present the synthesis, biological testing, and compound design. In addition, we postulate and assess computationally the binding mode for our inhibitors of p38 MAP kinase based on a 6,9-diarylpurine-8-one scaffold.

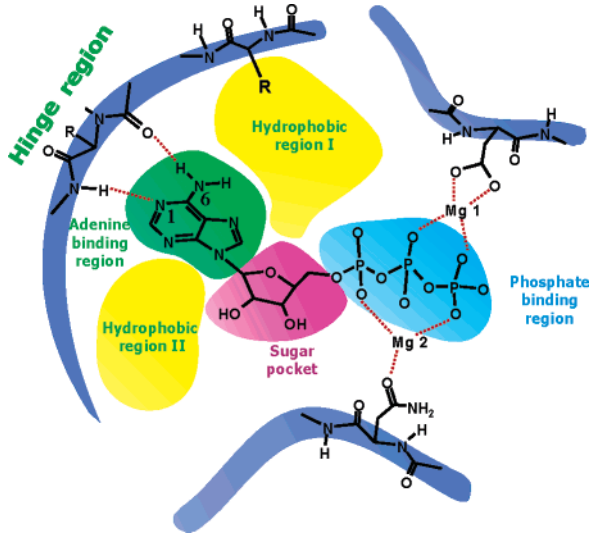

Figure 1. Mapping important regions within the ATP-binding-site of kinases based on both X-ray structures and computational methods (modified from Traxler[9]). The bidentate hydrogen-bond donor/acceptor system with the backbone of the hinge region anchors the ATP-adenine deep inside the binding cleft.

Scaffold Design for Targeting p38 MAP Kinase. Recently Wan et al.[11] published a series of *N*-phenyl-*N*-purin-6-yl ureas suggesting the design of directly derived adenine mimics. The backbone amide N−H of Met109 forms a conserved hydrogen bond even with structurally diverse ligands, e.g., (i) N-1 of ATP-adenine (Figure 1), (ii) the pyridine moiety of either SB 203580

* Author to whom correspondence should be addressed. Telephone: ++49 7071 2972459, fax: ++49 7071 295037, e-mail: stefan.laufer@uni-tuebingen.de.
[†] Eberhard-Karls-University Tübingen.
[‡] University Hospital Eberhard-Karls-University Tübingen.
[§] Benemérita Universidad Autónoma de Puebla.

[a] Abbreviations: p38 MAP kinase, p38 mitogen activated protein kinase; ATP, adenosine triphosphate; IL, interleukine; TNF, tumor necrose factor; FEB, free energy of binding; PI, predictive index.

10.1021/jm061061w CCC: $37.00
Published on Web 04/06/2007

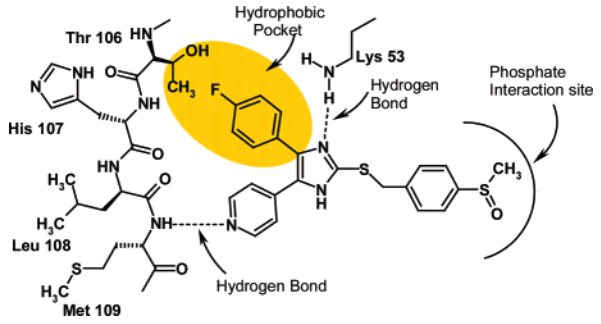

Figure 2. Schematic drawing of specific interactions between a pyridinylimidazole-based inhibitor (ML 3163) and the ATP binding site of p38 MAP kinase.[5] These are hydrogen bonds bridging the pyridine N-atom to backbone NH atoms of Met109 and the imidazole to the side chain of Lys53. The shaded area marks the interaction with hydrophobic region I with the role of a selectivity pocket for one aryl substituent. The ligand is docked in homology to SB203580 X-ray structure 1A9U.[8]

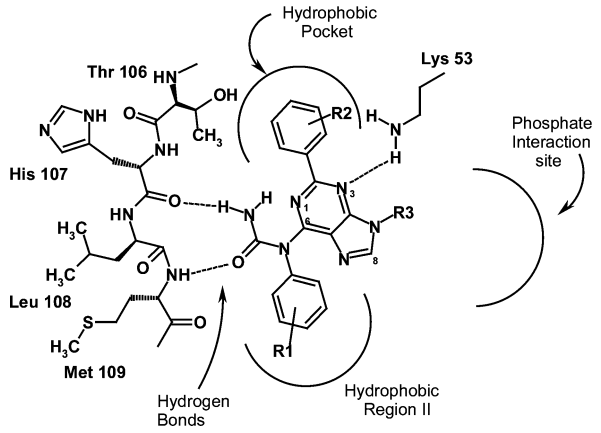

Figure 3. Schematic drawing of important interactions between urea-based inhibitors described by Wan[11] et al. and the ATP binding site of p38 MAP kinase, derived from X-ray crystallography.

or ML 3163 (Figure 2), and (iii) the urea oxygen of Wan's purine compounds (Figure 3). Another hydrogen bond between the amide carbonyl of His107 and the urea N−H on the ligand side is not generally conserved (Figure 3). Both hydrogen bonds mimic the bidentate hydrogen bond donor/acceptor system in the hinge region that anchors the adenine scaffold of ATP deeply inside the binding cleft. Like the 4-fluorophenyl moiety of ML 3163 (Figure 2), one phenyl ring in Wan's series occupies the hydrophobic region I (selectivity pocket) whereas another aromatic ring resides in hydrophobic region II; neither the pyridinyl-imidazole inhibitors nor ATP occupy this second hydrophobic site (Figure 3). Hence, affinity to the kinase increases. Both aryl moieties and the urea substructure are attached to a purine scaffold which in turn aligns the substituents to their appropriate spatial position in the binding cleft. This purine scaffold, however, does not directly contact the adenine binding region of the ATP-binding pocket, and the purine moiety is not part of the essential bidentate H-bonding system. Therefore, Wan's compounds cannot be seen as true adenine mimetics since such ingenious molecules should not only show the key interactions between an appropriately substituted purine or adenine and the backbone but also, ideally, bind within the adenine binding region of the ATP-binding pocket. Good examples in the literature that this goal can be achieved are the pyrazolo[3,4-*d*]pyrimidines PP1 and PP2 (Figure 4).[12,13] Their structure is closely related to adenine, and their N4 position corresponds to N6 position of ATP. When bound to Lck kinase

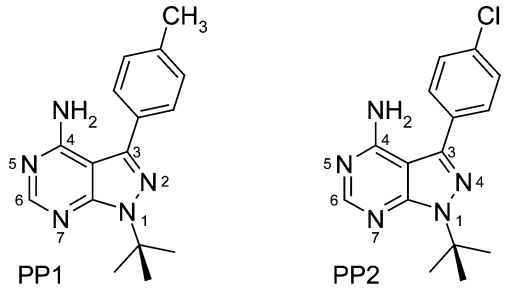

Figure 4. Chemical structures of PP1 and PP2.

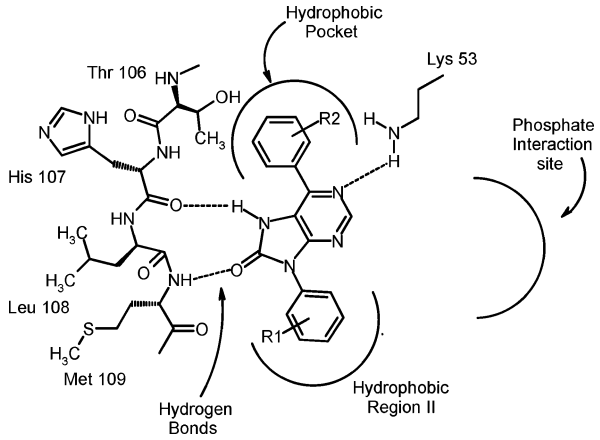

Figure 5. Schematic representation of the computed binding mode for our novel p38 MAP kinase inhibitors based on the 6,9-diarylpurin-8-one template. Important interactions between 6,9-diarylpurin-8-one-based inhibitors and the ATP binding site of p38 MAP kinase are displayed. The bidentate hydrogen bond donor/acceptor system with backbone atoms of the hinge region is achieved with these compounds as well.

(a member of the Src family), PP2 is nearly oriented as the adenine of bound ATP, and the chloroaromatic enters a lipophilic pocket (region I) opening behind N7.[14] PP1 and PP2 are strong inhibitors of kinases belonging to the Src family but were found to inhibit p38 MAP kinase as well.[15,16]

In the present study, our goal was to verify experimentally and computationally whether it would be possible to retain the aforementioned key features in aryl-substituted purine derivatives to create p38 MAP kinase inhibitors closely related to ATP. The *in silico* design assisted in scaffold optimization, binding mode prediction, and defining an appropriate substitution pattern to meet the geometrical features for the most advantageous interactions with the target protein.

We have therefore developed a series of 6,9-diarylpurin-8-ones consistent with the aforesaid requirements (Figures 5, 6). Compared to the compounds of Figure 3, the purine moiety is rotated clockwise about 120°, and a carbonyl function has been added at position 8, which brings about the hydrogen bond at N-7 (Figure 5). Consequently, the purine moiety is oriented back again to the adenine binding region, even though it assumes a horizontally flipped position compared to its orientation in kinase-bound ATP (see Figure 1). The aryl moieties are directly attached to positions C-6 and N-9 to extend to both hydrophobic regions I and II, respectively. The ortho mono- or disubstitution enforces a propeller-like conformation[11] of the aryl moieties for optimized interaction with either hydrophobic region.

We postulate that the essential interactions such as binding of the aryl moieties in hydrophobic regions I and II and the bidentate hydrogen bond donor/acceptor system with the backbone of the hinge region are conserved with our compound design.

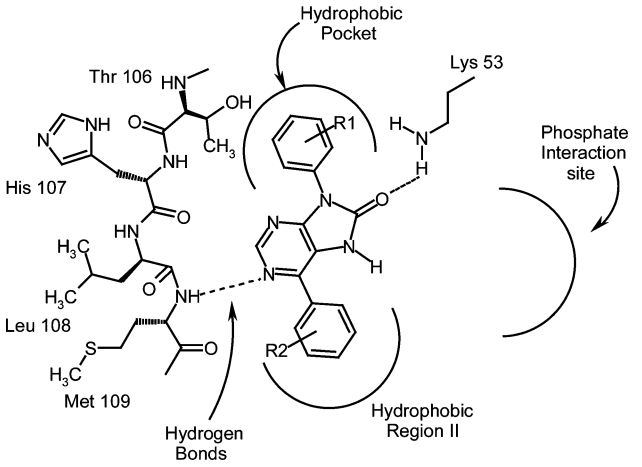

Figure 6. Schematic representation of the flipped binding mode for the 6,9-diarylpurin-8-one template derived from computational docking. The bidentate hydrogen bond donor/acceptor system with backbone atoms of the hinge region is not achieved in the flipped orientation. The formation of one hydrogen bond between the amide N−H of Met 109 and N1 of the purine is possible.

Scheme 1[a]

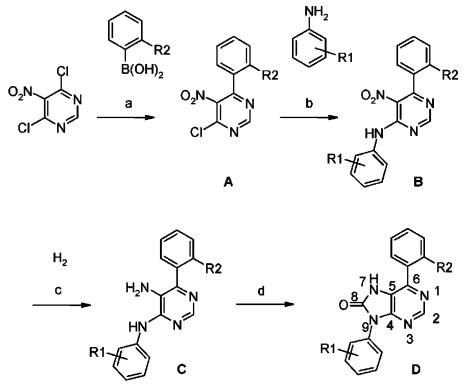

Compound D	preliminary product A	B	C	R2	R1
21	**1**	**4**	**12**	Cl	2,6-di-F
22	**1**	**5**	**13**	Cl	2,6-di-Me
23	**1**	**6**	**14**	Cl	2,4-di-F
24	**1** (R2=Cl)	**4** (R2=Cl)	**15** (R2=H)	H	2,6-di-F
25	**2**	**7**	**16**	Me	2,6-di-Me
26	**2**	**8**	**17**	Me	2,6-di-F
27	**2**	**9**	**18**	Me	2,4-di-F
28	**2**	**10**	**19**	Me	2,4-di-OMe
29	**3**	**11**	**20**	F	2,6-di-F
[b]**30**	**2**	**7**	**16**	Me	2,6-di-Me

[a] Reagents: (a) Appropriate boronic acid, K_2CO_3, toluene, $Pd(PPh_3)_4$, 90 °C; (b) appropriate aniline, triethylamine, THF, reflux; (c) PtS/C, H_2, 4 bar, EtOH, rt or Pd/C, H_2, 4 bar, EtOH, rt; (d) *N*,*N*-carbonyldiimidazole or *N*,*N*-thiocarbonyldiimidazole (for **30**) toluene/dioxane. [b]**30**: Purine-8-thione.

Charge distributions on oxygen and sulfur atoms at position C-8 show significant difference. A thio analogue of **25** (Scheme 1) is synthesized (**30**) for probing the loss of hydrogen-bonding in the activity tests. Isomeric structures are **21**/**23** and **26**/**27**. Since the purine is substituted with similar aryl moieties on opposite sides, the compounds show partial bilateral symmetry. Consequently we also expected answers about flip-flop[17] behavior from our docking studies.

Chemistry. A series of 6,9-diarylpurin-8-ones was synthesized according to an improved procedure described before.[18] The structurally related compounds presented by Cocuzza[18] et al. were reported as corticotropin-releasing hormone antagonists whereas their 8-oxo derivatives exhibited only weak antagonistic activity. Therefore, possible side effects of our 6,9-diarylpurin-8-ones should be minimized.

Table 1. Inhibition Data (IC_{50}, Enzyme Assay, ATP Concentration: 100 μM).

molecule ID number	IC_{50} (μM)
21	0.9
22	7.8
23	2.7
24	17.5
25	18.1
26	0.5
27	1.6
28	5.2
29	7.8
30	100
SB203580	0.056

Suzuki coupling reaction of ortho-substituted benzeneboronic acids with 4,6-dichloro-5-nitropyrimidine yielded the 6-aryl-4-chloro-5-nitro-pyrimidines **1**−**3** (see Scheme 1). Even with equimolar amounts of the reagents, the diarylated product was afforded as a minor side product. However, column chromatography easily separated the monoarylated pyrimidines, which eluted first (methylene chloride/hexane). Subsequent nucleophilic substitution of the remaining chlorine afforded the (6-aryl-5-nitro-pyrimidin-4-yl)-aryl-amines **4**−**11**. Reduction of the nitro group proceeded rapidly at ambient temperature with palladium on charcoal under a hydrogen atmosphere. However, these reduction conditions resulted in hydrodehalogenation in case of the chlorine-substituted aryls whereas fluorine compounds remained unaffected. The chlorine remained when platinum sulfide[19] on charcoal was used as the catalyst for hydrogenation, and the reduction of the nitro group proceeded as quickly as with palladium on charcoal. At this step the literature procedure[18] used an iron/acetic acid system in MeOH with refluxing. Our more versatile procedure gave nearly quantitative yields of the diarylpyrimidinediamines **12**−**20**. For the following ring closure the literature procedure[18] employed phosgene in toluene under reflux conditions. The highly volatile and toxic phosgene could be easily replaced by *N*,*N*-carbonyldiimidazole[20] which afforded the diarylpurin-8-ones in good yields and with short reaction times.

NMR Studies. To evaluate the rotational barrier of the ortho monosubstituted aryl moiety at C-6 of the purin-8-one we have performed temperature-dependent NMR measurements. As samples we chose **24** with its freely rotateable phenyl group and **26** with the ortho methyl-substituted phenyl. Following Wan's argument, the aryl at C-6 should bind deeply inside the lipophilic selectivity pocked. Therefore a propeller-like conformation of the C-6 aryl would be favorable. In the NMR studies we did not see any change in the signal line width upon the rotational barrier (see spectra in the Supporting Information). So we conclude a rotational barrier between 7.1 and 10.7 kcal/mol which is in agreement with literature data.[21,22] This would mean that in solution and at a temperature relevant for biological systems the aryl would be somewhat rotateable at least over the N-1 of the purine scaffold, allowing it to rotate to a favored position which would allow the entry into the binding pocket in the sense of an induced fit. The ortho substituent should facilitate this as already stated by Wan et al. This finding is consistent with the difference of the inhibition values of **24** and **26**.

Biological Testing. The compounds which widely followed the favorable substitution pattern found by Wan et al. were tested with a recently published non-radioactive enzyme assay.[23] The test results are shown in Table 2. SB203580 is a widely utilized

Table 2. Free Energy of Binding (FEB) by Autodock versus Experimental Affinity Data for Three Sets of Docked Conformations of the Purin-8-one Derivatives.

molecule ID no.	IC_{50} (μM)	FEB of best solutions (kcal/mol)	FEB of orientation 1 (kcal/mol)	FEB of orientation 2 (kcal/mol)
21	0.9	−8.7	−8.7	−8.7
22	7.8	−9.4	−9.4	−9.2
23	2.7	−8.8	−8.8	−8.7
24	17.5	−8.2	−8.2	−8.2
25	18.1	−9.4	−9.4	−8.0
26	0.5	−8.8	−8.7	−8.8
27	1.6	−8.9	−8.7	−8.9
28	5.2	−9.2	−8.8	−9.2
29	7.8	−8.5	−8.5	−6.9
30	100	−9.4	−9.2	−9.4

reference substance in p38 MAP kinase research and served as a standard in our testing. The IC_{50} of our best compound was 1 order of magnitude higher than that of SB203580. As Wan et al. gave no data for a literature known reference compound, a direct comparison of our compounds with Wan's is not possible. We performed molecular modeling calculations to evaluate if it would be possible to find a proof for our envisioned binding mode (Figure 5) which followed the binding mode proposed by Wan (Figure 3).

Molecular Modeling. Until now, the coordinates of Wan's crystal structure were not published in the PDB. Therefore we chose PDB entry 1OVE[24] as the rigid receptor model because of its good resolution and a structural similarity of the diaryl-substituted 3,4-dihydro-1*H*-quinolin-2-one with our diaryl-substituted purin-8-one scaffold. Morever, the carbonyl group is located in a position that corresponds closely to that found in the purin-8-ones. The missing side chain atoms of Arg173 were added. Each ligand was built with MOE[25] and minimized using MMFF94 force field[26] with standard set up. For the ligands, Gasteiger charges[27] were calculated using Autodock Tools (MGL Tools 1.3alpha2[28,29]). The receptor model was prepared with Autodock Tools, deleting all water molecules, adding polar hydrogens and loading Kollman United Atoms charges.[30] We set the following parameters and options: sample numbers 256; survival rate 3; grid position and resolution 0.5; bond rotation 10°; translation step size 1; cluster width 2.5, using the GALS algorithm[31] until the ligand position was uniquely reproduced among the top hundred conformers with lowest free energies (−12 kcal/mol). Autodock 3 allows fast docking (100 conformations in 70 min of CPU time on a standard PC with AMD Athlon 2.4 GHz CPU running Red Hat Linux 9). Except for **28** with four rotatable bonds, the series were treatable with just two rotatable bonds between the scaffold and the aryl substitutions. FlexX docking was performed using FlexX v.1.13.5 as implemented in Sybyl 7.0.[32] FlexX was approximately 10 times faster than Autodock 3 and therefore is better qualified for docking large compound libraries.

Results and Discussion

Autodock 3 and FlexX are docking programs capable of predicting the binding geometry found in the crystallographic complex 1OVE[24] (RMSD = 0.9 Å). As stated above 1OVE was chosen as a reference to verify simulation because it reflects well the structural pattern of our test series. (Figure 7).

The Autodock 3 program is better suited to explore the unknown binding mode of our series, as it geometrically places all ligands in the same cavities occupied by the cocrystallized ligand of 1OVE (Figure 8). In contrast to the concise picture Autodock 3 provides, FlexX only yields dispersed poses in the cleft, due to its fragment-based search algorithm. As a result, it becomes more difficult to decide which of the many conformations is of binding relevance (Figure 9).

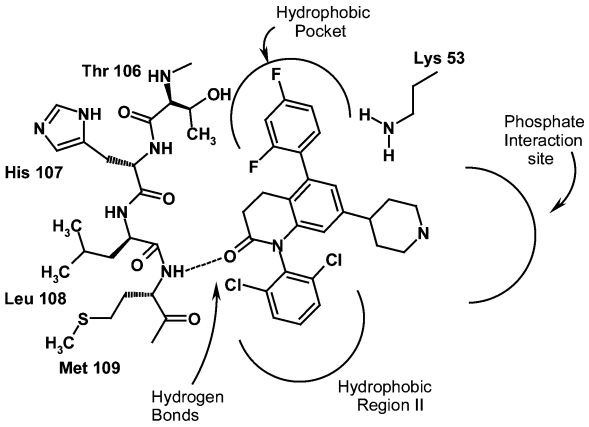

Figure 7. Schematic drawing of the 3,4-dihydro-1*H*-quinolin-2-one-based inhibitor from X-ray structure 1OVE.[24] This pdb entry served as template for docking studies. (IC_{50} = 0.74 nM at 2 μM ATP).

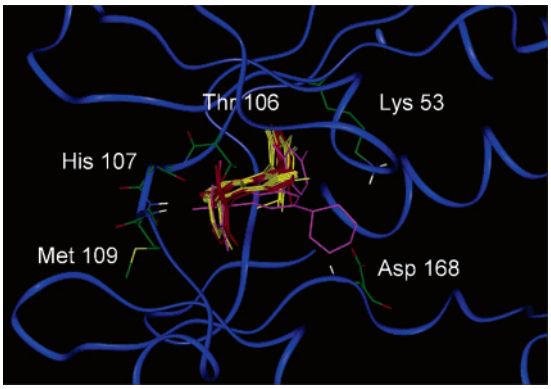

Figure 8. Docking results obtained using Autodock 3. All purin-8-ones bind in a position similar to that of the cocrystallized compound as reference (magenta) but show two orientations. Orientation **1** (red) cf. Figure 5 with the oxygen pointing at Met109 and the 180° flipped orientation **2** (yellow) cf. Figure 6 with the oxygen pointing at Lys53.

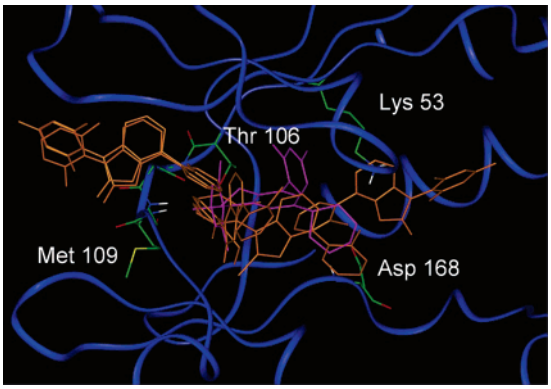

Figure 9. Docking of our purin-8-ones (orange) into the ATP binding site of p38 Map kinase (PDB entry 1ove) using FlexX. Important amino acids are colored by atom type. The cocrystallized compound as reference is colored magenta. Figures 8 and 9 were generated with InsightII.[46]

It is possible to separate the docking results of Autodock 3 into two groups which are referred to as orientation 1 and the flipped orientation 2: In orientation 1 (Figure 5 and red molecules in Figure 8) each ligand bears the possibility of forming a bidentate hydrogen bond donor/acceptor system with the hinge region of the kinase. A third hydrogen bond may be formed between N-1 of the purine and Lys53. Orientation 2

Table 3. Predictive Indices (PI) of Different Docking-Scoring Combinations. The Higher the PI Value the More Accurate Is the Prediction for Significant Inhibitor Ranking against Mere Random Distribution (PI = 0).

scoring	Autodock best solution	Autodock orientation 1	Autodock orientation 2	Chem-score	D score	F score	G score	PMF score
Autodock	−0.46	−0.27	−0.17					
Chem score	−0.53	−0.19	−0.32	−0.27	−0.27	−0.26	−0.19	−0.38
D score	−0.54	−0.32	−0.38	−0.22	−0.22	−0.28	−0.14	0.46
F score	0.36	0.55	0.73	−0.07	−0.07	0.03	−0.06	−0.32
G score	−0.55	−0.37	−0.33	−0.25	−0.25	−0.25	−0.14	−0.04
PMF score	0.09	0.19	0.08	0.24	0.24	0.51	0.36	0.42

(Figure 6 and yellow molecules in Figure 8) allows the putative formation of a single hydrogen bond between the amide N−H of Met109 and N-1 of the purine. In this orientation Lys53 may form a hydrogen bond with C-8 carbonyl oxygen. Table 2 presents a comparison between the calculated energies and the experimentally determined IC_{50} values. Orientations 1 and 2 show minor differences in terms of free energies of binding (FEB) as calculated using Autodock 3 (0.04−1.63 kcal/mol). Since the estimated FEB values vary over the narrow range from −8.24 to −9.44 kcal/mol, no significant ranking of the different inhibitors of our series can be performed which could reflect the ranking of the IC_{50} values. Furthermore no commitment to orientation 1 or 2 is possible. To improve the dissatisfying scoring by Autodock 3, the scoring functions available in the Sybyl Cscore module were applied to the three subsets of Autodock 3 conformations shown in columns 3−5 in Table 2. These scoring functions are **(**1**)** The FlexX scoring function,[33] (2) The PMF scoring function,[34] (3) The Dock scoring function,[35] (4) the Chemscore scoring function,[36] and (5**)** the GOLD scoring function.[37] The predictive index (PI) introduced by Pearlman[38] is used to assess the capability of each scoring function to predict the ranking of the inhibitors. The results are shown in the first three columns of Table 3 and discussed below. For a set of experimental pK_i (or pIC_{50}) values, $E(i)$, and corresponding predicted scores $P(i)$ the predictive index (PI) is defined as follows:[38]

$$\mathrm{PI} = \sum_{j>i}\sum_{i} w_{ij}\, C_{ij} / \sum_{j>i}\sum_{i} w_{ij} \tag{1}$$

with

$$w_{ij} = |E(j) - E(i)| \tag{2}$$

and

$$C_{ij} = \begin{cases} 1 & \text{if } [E(j) - E(i)]/[P(j) - P(i)] < 0 \\ -1 & \text{if } [E(j) - E(i)]/[P(j) - P(i)] > 0 \\ 0 & \text{if } [P(j) - P(i)] = 0 \end{cases} \tag{3}$$

$P(i)$ is the model score assigned to molecule i, and $E(i)$ is the experimental pIC_{50}. This index ranges from −1 to +1, depending on how well the predictions track the order of experiment: +1 arises from perfect prediction, −1 arises from predictions that are always wrong, and 0 arises from predictions that are completely random. This function includes a weighting term that depends on the difference between the experimental values which in turn reflects the fact that a good function should be able to differentiate between changes that result in large differences in binding.

As an additional approach to compare the performance of the five scoring functions mentioned above, we used each of them to determine the docked position of each molecule. For this purpose 600 docked conformations were generated of each molecule using FlexX as the docking engine. Then each of the scoring functions was used to select the best of the 600 conformations of every molecule. This results in five sets of conformations of each of the ten molecules. Each of the five scoring functions was applied to these five sets of docking results and once more ranked by the other four scoring functions. Again the PI is used to assess the concordance between the ranking by each scoring function and the IC_{50}. Table 3 (columns 4−8) shows the PI results of the different combinations of docking methods and scoring functions. Most of the combinations show results that are random. Only the combination of the five docking methods with PMF score yields always a positive PI which means a better prediction. Columns 1−3 show the PI results for the combination of the three sets of Autodock conformations with the different scoring functions including the Autodock scores in row 1. The scoring of orientation 2 obtained by Autodock 3 alternatively using the FlexX scoring function attains the highest predictive index (PI = 0.73). Applying the FlexX scoring function to orientation 1 results in an inhibitor ranking which is still significantly better than random distribution (PI = 0.55). For the lowest energy Autodock 3 conformations, the highest PI is again obtained by using the FlexX scoring function (PI = 0.36). The other docking/scoring combinations do not generate better results.

We examined the H-bonding properties of diarylpurin-8-ones and diarylpurine-8-thiones. The calculated difference between the Autodock 3 scores of **25** and its thio analogue **30** does not correspond to the observed difference in their biological activities. Compared to oxygen (EN = 3.5), sulfur is less electronegative (EN = 2.4), and hence a relatively more positive charge can be expected. To evaluate the electrostatic influence on the score ranking, we tried several thio models by modifying the partial charges of sulfur (e.g.: Gasteiger Marsili: −0.05 vs MMFF94: −0.40) and its adjacent carbon atom (Gasteiger Marsili: +0.17 vs MMFF94: +0.50) adjusting charges for electroneutrality.[26,27] Since no significant improvement of sensitivity could be observed, we conducted AM1-based semiempirical MOPAC[39] calculations with full geometry optimization to increase the precision level of the electronic description of "oxo" and "thio" groups as potential hydrogen-bond acceptors. The rationale behind the decision to select the AM1 Hamiltonian among current quantum-chemical methods is supported by the literature.[39−43] The computed charges revealed that there is significantly more negative net atomic partial charge on the oxygen atom (−0.32) of **25** than on the equilocated sulfur atom (−0.25) of **30.** This means for oxygen and sulfur, respectively, any increase in the net atomic partial charge decreases of the potential to build up hydrogen bonds for homologous O or S dotted series. Thio analogues are less potent H-bond acceptors and form a weaker H-bond than that of the 6,9-diarylpurin-8-ones, which clearly correlates with the experimentally observed loss in binding affinity (Table 2). This is consistent with the data published by Masunov and Dannen-

berg for urea (−30 to −40 kJ/mol) and thiourea (−20 to −30 kJ/mol) dimerization energies.[44]

Conclusion

The binding mode of inhibitors in the ATP binding site of p38 MAP kinase is determined by both hydrogen bonds and lipophilic interactions. Computational methods to predict the ranking of biological activities of different inhibitors should balance both types of interaction. Autodock 3[31] performs well in the case of p38 MAP kinase giving similar docking results for the structurally similar inhibitors of our purin-8-one series. In good agreement with the reference complex, 1OVE, the hydrophobic aryl moieties fit tightly into the hydrophobic pockets. On one hand, Autodock predicts favorable geometries but on the other hand the binding energies calculated by Autodock 3 reflect only partially the ranking of all inhibitors. In contrast the docking program FlexX does not predict a consistent binding mode but scatters all molecules over the binding site due to its fragment-based cavity exploration and its overemphasis on hydrogen bond contacts during the docking process.[45] Nonetheless, the FlexX scoring function is most valuable to predict the ranking of biological activities among inhibitors. The predictive index of 0.73 achieved by the combination of Autodock docking geometries with FlexX scoring is close to perfect prediction of the inhibitor ranking. In analogy to Wan et al.[11] we designed a diarylpurin-8-one scaffold with a very similar binding mode which includes two possible orientations of the central purin-8-one scaffold. The first of the orientations allows the formation of a bidentate H-bond network with the conserved hydrogen bonds to Met109 and adjacent His107 in complete pharmacophoric equivalency to the known ATP binding while orientation 2 allows only a single conserved hydrogen bond to Met109. Moreover the binding feature of the two aryl moieties is in good agreement with the structural requirements described in the literature which are represented by the cocrystallized molecule of the template 1OVE. With both orientations of the purin-8-one scaffold, the aryl moieties are able to address not only the hydrophobic region I as already observed in complexed SB 203580[8] but additionally the hydrophobic region II. The ortho substituents of the aromatic moieties may force them into a twisted position relative to the plane of the purine scaffold, resulting in the earlier described propeller-like conformations.[11] This allows an optimal access of the purine C-6 aryl group to hydrophobic region I (pocket) and improved interaction between the second aryl (N-9) and hydrophobic region II which is formed by the surfaces above and below the ATP-adenine at the point where the binding cleft opens to the solvent. The methyl group of the most active compound **26** is optimally buried by the lipophilic side chains of Val38, Ala51, and Lys53 (Figure 10, showing **26** in orientation 1).

New synthetic work will be directed toward derivatization of the scaffold and side chains. The combination of different computational methods, e.g., the docking geometries from Autodock and the scoring by FlexX allows to eliminate possible poor candidates prior to synthetic attempts. Consequently, it is possible to focus on the most promising candidates for further improvement of the affinity of purine derivatives to p38 MAP kinase. We were able to compute two possible binding modes for our new purine series with ligand docking studies and verify the model by reference to a related crystal structure and to rate possible conformations by means of Pearlman's predictive index. This model contributes new and promising aspects for future drug development cycles regarding the competitive inhibition of ATP-consuming enzymes.

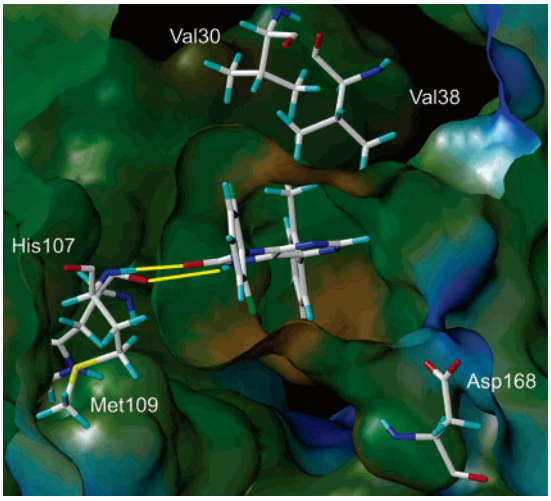

Figure 10. The most active compound **26** docked into the ATP binding site of p38 MAP kinase. The solvent-accessible surface[47] is calculated using the Molcad module of Sybyl 7.0[32] and colored by lipophilicity[48] (brown = lipophilic, blue = hydrophilic). The *o*-methyl group is in optimal interaction with the hydrophobic region formed by the side chains of Val30 and Val38. Important hydrogen bonds with the backbone of Met109 and His107 are marked by yellow lines.

Experimental Section

Chemistry. All reagents and solvents were of commercial quality and used without further purification. General procedures for the preparation of compounds **A**−**D** (find procedures and spectroscopic data for the particular compounds in Supporting Information):

General Procedure A for the Preparation of 4-Chloro-5-nitro-6-phenyl-pyrimidines (1−3). A mixture of 4,6-dichloro-5-nitro-pyrimidine (1 equiv), the appropriate benzeneboronic acid (1.1 equiv), K_2CO_3 (1.25 equiv), $Pd(PPh_3)_4$ (0.01−0.02 equiv), and a sufficient amount of toluene was stirred under argon, protected from light at 90 °C for 5−9 h. The mixture was cooled to ambient temperature and filtered and the residue washed with dry ethanol. The filtrate was evaporated *in vacuo* and the viscous residue purified by column chromatography (SiO_2 60, CH_2Cl_2/hexane 8:2) to afford **1**−**3**.

General Procedure B for the Preparation of (5-Nitro-6-phenyl-pyrimidin-4-yl)-phenyl-amines (4−11). The appropriate 4-chloro-5-nitro-6-phenyl-pyrimidines **A** were refluxed together with the suitable anilines (1.5−4 equiv) and triethylamine (1.5−4 equiv) in dioxane for 7−10 h. The volatiles were evaporated *in vacuo*, and the residue was crystallized from cyclohexane. The crystals were collected and dissolved in CH_2Cl_2, and the solution was filtered over SiO_2 using CH_2Cl_2 as eluent. The filtrate was evaporated *in vacuo* to afford **4**−**11**.

General Procedure C for the Preparation of 6-(Aryl)-N'4'-(aryl)-pyrimidine-diamines (12−20). The appropriate (5-nitro-6-phenyl-pyrimidin-4-yl)-phenyl-amines **B** were dissolved in ethanol, palladium on charcoal (Pd−C, 10% on charcoal) or sulfidated platinum on charcoal (PtS−C, 5% on charcoal) in case of **12** and **13** was added, and the mixture stirred at ambient temperature for 30 min at a hydrogen pressure of 4 bar. The mixture was filtered, and the volatiles were evaporated *in vacuo* to afford **12**−**20**.

General Procedure D for the Preparation of 6,9-Diaryl-purine-8-ones (21−29). The appropriate 6-(Aryl)-N'4'-(aryl)-pyrimidine-diamines **C** and *N*,*N*-carbonyldiimidazole were dissolved in a mixture of dioxane and toluene, and the mixture was refluxed for 2.5−6 h. The volatiles were evaporated *in vacuo*, and the residue was purified by column chromatography (SiO_2 60, toluene/acetone 8:2) to afford **21**−**29**.

Acknowledgment. We thank Klaus Albert and his co-workers for the execution of the temperature-dependent NMR

experiments. The authors are grateful to Sabine Luik for assistance in biological testing and would like to thank Merckle GmbH, Ulm, Germany, and Fonds der Chemischen Industrie, Germany, for their generous support of this work. Also thanks are given to Hossam Elgabarty for discussion.

Supporting Information Available: Experimental procedures, spectroscopic data, table of elemental analyses, and temperature-dependent NMR spectra for **24** and **26**. This material is available free of charge via the Internet at http://pubs.acs.org.

References

(1) Kumar, S.; Boehm, J.; Lee, J. C. p38 MAP kinases: key signalling molecules as therapeutic targets for inflammatory diseases. *Nat. Rev. Drug Discovery* **2003**, *2*, 717−726.
(2) Johnson, G. L.; Lapadat, R. Mitogen-activated protein kinase pathways mediated by ERK, JNK, and p38 protein kinases. *Science* **2002**, *298*, 1911−1912.
(3) Smolen, J. S.; Steiner, G. Therapeutic strategies for rheumatoid arthritis. *Nat. Rev. Drug Discovery* **2003**, *2*, 473−488.
(4) Jackson, P. F.; Bullington, J. L. Pyridinylimidazole based p38 MAP kinase inhibitors. *Curr. Top. Med. Chem* **2002**, *2*, 1011−1020.
(5) Laufer, S. A.; Wagner, G. K. From Imidazoles to Pyrimidines: New Inhibitors of Cytokine Release. *J. Med. Chem.* **2002**, *45*, 2733−2740.
(6) Cohen, P. The development and therapeutic potential of protein kinase inhibitors. *Curr. Opin. Chem. Biol.* **1999**, *3*, 459−465.
(7) Bellon, S.; Fitzgibbon, M. J.; Fox, T.; Hsiao, H. M.; Wilson, K. P. The structure of phosphorylated p38gamma is monomeric and reveals a conserved activation-loop conformation. *Structure Fold. Des.* **1999**, *7*, 1057−1065.
(8) Wang, Z.; Canagarajah, B. J.; Boehm, J. C.; Kassisa, S.; Cobb, M. H.; Young, P. R.; Abdel-Meguid, S.; Adams, J. L.; Goldsmith, E. J. Structural basis of inhibitor selectivity in MAP kinases. *Structure* **1998**, *6*, 1117−1128.
(9) Traxler, P. Tyrosine kinase inhibitors in cancer treatment (part II). *Expert Opin. Ther. Pat.* **1998**, *8*, 1599−1625.
(10) Laufer, S. A.; Domeyer, D. M.; Scior, T. R.; Albrecht, W.; Hauser, D. R. Synthesis and biological testing of purine derivatives as potential ATP-competitive kinase inhibitors. *J. Med. Chem.* **2005**, *48*, 710−722.
(11) Wan, Z.; Boehm, J. C.; Bower, M. J.; Kassis, S.; Lee, J. C.; Zhao, B.; Adams, J. L. N-Phenyl-N-purin-6-yl ureas: The design and synthesis of p38a MAP kinase inhibitors. *Bioorg. Med. Chem. Lett.* **2003**, *13*, 1191−1194.
(12) Hanke, J. H.; Gardner, J. P.; Dow, R. L.; Changelian, P. S.; Brissette, W. H.; Weringer, E. J.; Pollok, B. A.; Connelly, P. A. Discovery of a novel, potent, and Src family-selective tyrosine kinase inhibitor. Study of Lck- and FynT-dependent T cell activation. *J. Biol. Chem.* **1996**, *271*, 695−701.
(13) Liu, Y.; Bishop, A.; Witucki, L.; Kraybill, B.; Shimizu, E.; Tsien, J.; Ubersax, J.; Blethrow, J.; Morgan, D. O.; Shokat, K. M. Structural basis for selective inhibition of Src family kinases by PP1. *Chem. Biol.* **1999**, *6*, 671−678.
(14) Zhu, X.; Kim, J. L.; Newcomb, J. R.; Rose, P. E.; Stover, D. R.; Toledo, L. M.; Zhao, H.; Morgenstern, K. A. Structural analysis of the lymphocyte-specific kinase Lck in complex with non-selective and Src family selective kinase inhibitors. *Structure* **1999**, *7*, 651−661.
(15) Bain, J.; McLauchlan, H.; Elliott, M.; Cohen, P. The specificities of protein kinase inhibitors: an update. *Biochem. J.* **2003**, *371*, 199−204.
(16) Cohen, P.; Goedert, M. Engineering protein kinases with distinct nucleotide specificities and inhibitor sensitivities by mutation of a single amino acid. *Chem. Biol.* **1998**, *5*, R161−R164.
(17) Doytchinova, I.; Petrova, S. \"N6−N7\" - a modification of the \"N6−C8\" model for the binding site on adenosine A1 receptors with improved steric and electrostatic fit. *Med. Chem. Res.* **1998**, *8*, 143−152.
(18) Cocuzza, A. J.; Chidester, D. R.; Culp, S.; Fitzgerald, L.; Gilligan, P. Use of the Suzuki reaction for the synthesis of aryl-substituted heterocycles as corticotropin-releasing hormone (CRH) antagonists. *Bioorg. Med. Chem. Lett.* **1999**, *9*, 1063−1066.
(19) Davoll, J. Pyrrolo[2,3-d]pyrimidines. *J. Chem. Soc., Abstr.* **1960**, 131−138.
(20) Staab, H. A. Syntheses with heterocyclic amides (azolides). *Angew. Chem.* **1962**, *74*, 407−23.
(21) Mazzanti, A.; Lunazzi, L.; Minzoni, M.; Anderson, J. E. Rotation in biphenyls with a single ortho-substituent. *J. Org. Chem.* **2006**, *71*, 5474−5481.
(22) Bott, G.; Field, L. D.; Sternhell, S. Steric effects. A study of a rationally designed system. *J. Am. Chem. Soc.* **1980**, *102*, 5618−5626.
(23) Laufer, S.; Thuma, S.; Peifer, C.; Greim, C.; Herweh, Y.; Albrecht, A.; Dehner, F. An immunosorbent, nonradioactive p38 MAP kinase assay comparable to standard radioactive liquid-phase assays. *Anal. Biochem.* **2005**, 135−137.
(24) Fitzgerald, C. E.; Patel, S. B.; Becker, J. W.; Cameron, P. M.; Zaller, D.; Pikounis, V. B.; O'Keefe, S. J.; Scapin, G. Structural basis for p38a MAP kinase quinazolinone and pyridol-pyrimidine inhibitor specificity. *Nat. Struct. Biol.* **2003**, *10*, 764−769.
(25) MOE. Chemical Computing Group Inc. Montreal, 2004.
(26) Halgren, T. A. Maximally diagonal force constants in dependent angle-bending coordinates. II. Implications for the design of empirical force fields. *J. Am. Chem. Soc.* **1990**, *112*, 4710−4723.
(27) Gasteiger, J.; Marsili, M. Prediction of proton magnetic resonance shifts: the dependence on hydrogen charges obtained by iterative partial equalization of orbital electronegativity. *Org. Magn. Reson.* **1981**, *15*, 353−360.
(28) Sanner, M. F. Python: A programming language for software integration and development. *J. Mol. Graphics Modell.* **1999**, *17*, 57−61.
(29) Michel, F. Sanner; Daniel Stoffler; Arthur, J. Olson ViPEr a Visual Programming Environment for Python. Presented at the 10th International Python Conference, Feb 4−7, 2002. (http://www.scripps.edu/~sanner/html/papers/IPC02.pdf).
(30) Weiner, S. J.; Kollman, P. A.; Nguyen, D. T.; Case, D. A. An all atom force field for simulations of proteins and nucleic acids. *J. Comput. Chem.* **1986**, *7*, 230−252.
(31) Morris, G. M.; Goodsell, D. S.; Halliday, R. S.; Huey, R.; Hart, W. E.; Belew, R. K.; Olson, A. J. Automated docking using a Lamarckian genetic algorithm and an empirical binding free energy function. *J. Comput. Chem.* **1998**, *19*, 1639−1662.
(32) Sybyl 7.0. Tripos Inc. St.Louis, MO, 2004.
(33) Rarey, M.; Kramer, B.; Lengauer, T.; Klebe, G. A fast flexible docking method using an incremental construction algorithm. *J. Mol. Biol.* **1996**, *261*, 470−489.
(34) Muegge, I.; Martin, Y. C. A General and Fast Scoring Function for Protein-Ligand Interactions: A Simplified Potential Approach. *J. Med. Chem.* **1999**, *42*, 791−804.
(35) Kuntz, I. D.; Blaney, J. M.; Oatley, S. J.; Langridge, R.; Ferrin, T. E. A geometric approach to macromolecule-ligand interactions. *J. Mol. Biol.* **1982**, *161*, 269−288.
(36) Eldridge, M. D.; Murray, C. W.; Auton, T. R.; Paolini, G. V.; Mee, R. P. Empirical scoring functions: I. The development of a fast empirical scoring function to estimate the binding affinity of ligands in receptor complexes. *J. Comput.-Aided Mol. Des.* **1997**, *11*, 425−445.
(37) Jones, G.; Willett, P.; Glen, R. C.; Leach, A. R.; Taylor, R. Development and validation of a genetic algorithm for flexible docking. *J. Mol. Biol.* **1997**, *267*, 727−748.
(38) Pearlman, D. A.; Charifson, P. S. Are free energy calculations useful in practice? A comparison with rapid scoring functions for the p38 MAP kinase protein system. *J. Med. Chem.* **2001**, *44*, 3417−3423.
(39) Dewar, M. J. S.; Zoebisch, E. G.; Healy, E. F.; Stewart, J. J. P. Development and use of quantum mechanical molecular models. 76. AM1: a new general purpose quantum mechanical molecular model. *J. Am. Chem. Soc.* **1985**, *107*, 3902−3909.
(40) Stewart, J. J. P. Semiempirical molecular orbital methods. In *Reviews in Computational Chemistry*; VCH Publishers: New York, 1990; Volume 1, pp 45−81
(41) Nowak, W.; Wietzbowska, M. A theoretical study of geometry and transition moment directions of flexible fluorescent probes - Acetoxy derivatives of phenylanthracene. *THEOCHEM* **1996**, *368*, 223−234.
(42) Testa, A. C. Hydrogen bonding and the protonated water dimer. *Spectrosc. Lett.* **1999**, *32*, 819−828.
(43) Bures, M.; Bezus, J. Study of hydrogen bonding in carboxylic acids by the MNDO/M method. *Collect. Czech. Chem. Commun.* **1994**, *59*, 1251−1260.
(44) Masunov, A.; Dannenberg, J. J. Theoretical study of urea and thiourea. 2. Chains and ribbons. *J. Phys. Chem. B* **2000**, *104*, 806−810.
(45) Stahl, M.; Rarey, M. Detailed Analysis of Scoring Functions for Virtual Screening. *J. Med. Chem.* **2001**, *44*, 1035−1042.
(46) InsightII 2000. Accelrys Inc. San Diego, CA, 2000.
(47) Connolly, M. L. Solvent-accessible surfaces of proteins and nucleic acids. *Science* **1983**, *221*, 709−713.
(48) Ghose, A. K.; Viswanadhan, V. N.; Wendoloski, J. J. Prediction of hydrophobic (lipophilic) properties of small organic molecules using fragmental methods: An analysis of ALOGP and CLOGP methods. *J. Phys. Chem. A* **1998**, *102*, 3762−3772.

JM061061W